Desalination and Water Treatment
www.deswater.com

doi: 10.1080/19443994.2016.1184187

57 (2016) 29488–29499
December

Taylor & Francis
Taylor & Francis Group

Adsorptive removal of phenol from aqueous solution on a modified palm shell-based carbon: fixed-bed adsorption studies

Abdurrahman Garba[a], Noor Shawal Nasri[b,c,*], Hatijah Basri[a], Razali Ismail[d], Zulkifli Abdul Majid[b], Usman D. Hamza[b,c,e,f], Jibril Mohammed[b,c,e,f]

[a]*Faculty of Science, Technology and Human Development, Department of Science, University Tun Hussein Onn Malaysia, Parit Raja, Batu Pahat, Johor 86400, Malaysia, Tel. +2348033617046; emails: agarba2008@yahoo.com, agarba2008@gmail.com (A. Garba), Tel. +60127704630; email: hatijah@uthm.edu.my (H. Basri)*

[b]*UTM-MPRC Institute for Oil and Gas, Resource Sustainability, Research Alliance, Research University, Universiti Teknologi Malaysia, Johor Bahru 81300 UTM, Johor, Malaysia, Tel. +60137728200; email: noorshaw@petroleum.utm.my (N.S. Nasri), Tel. +60197407602; email: zulmajid@petroleum.utm.my (Z. Abdul Majid), Tel. +2348023635827; email: usmandhamza@yahoo.com (U.D. Hamza), Tel. +2348104893452; email: jibrilmuhammad@yahoo.com (J. Mohammed)*

[c]*Faculty of Petroleum and Renewable Energy Engineering, Renewable Energy Engineering Department, University Teknologi Malaysia, Johor Bahru 81300 UTM, Johor, Malaysia*

[d]*Faculty of Science, Chemistry Department, Universiti Teknologi Malaysia, Skudai 81310, Johor Bahru, Malaysia, Tel. +60167580715; email: zali@kimia.fs.utm.my*

[e]*Faculty of Chemical Engineering, Chemical Engineering Department, Research University, Universiti Teknologi Malaysia, Johor Bahru, Johor, Malaysia*

[f]*Chemical Engineering Department, Abubakar Tafawa Balewa University, Tafawa Balewa Way, Bauchi PMB 0248, Bauchi State, Nigeria*

Received 17 December 2015; Accepted 23 April 2016

ABSTRACT

In this study, activated carbon from oil palm shell was produced by two-step chemical activation using K_2CO_3 as the chemical activant in the ratio 1:2 for the removal of phenol in a fixed-bed column. The characterization of the carbon was carried by Fourier Transform Infrared spectroscopy, Scanning electron microscope, thermogravimetric analysis, zeta potential, Brunauer–Emmett–Teller (BET) surface area, Elemental and Proximate analysis. The Langmuir surface area, BET surface area, and pore volume of the carbon were 817 m^2/g, 707 m^2/g, and 0.31 cm^3/g, respectively. The examination of several factors including bed depth, initial phenol concentration, and flow rate were carried out at constant pH of 6.5. The maximum sorption capacity of the carbon for phenol was 238.12 at 250 mg/L initial phenol concentration, 1 cm bed depth, and 9 mL/min flow rate. Thermodynamic parameters were determined to analyze the behavior of phenol uptake at different temperatures. Breakthrough curve models indicated that Yoon–Nelson model fitted the experimental data better than Adams–Bohart and Thomas models. According to the results obtained, activated carbon prepared from oil palm shell, modified with ammonia solution was an effective, sustainable, low cost, and alternative adsorbent for the removal of phenol in aqueous solutions.

*Corresponding author.

Presented at the 8th International Conference on Challenges in Environmental Science & Engineering (CESE-2015) 28 September–2 October 2015, Sydney, Australia

Keywords: Adsorption; Phenol; Potassium carbonate; Chemical activation; Activated carbon

1. Introduction

In recent times, industrial and agricultural developments coupled with rapid population growth reduced the quality of clean water resources due to indiscriminate disposal of hazardous waste which contaminates both ground and surface water. Phenol and phenolic derivatives are considered to be one of the foremost pollutants in wastewater. They are found in effluents from petrochemical, pharmaceutical, cosmetic, wood processing, plastic, pesticide, textile, steel, rubber, dye, paper, and pulp industries [1–3]. Wastewaters containing phenolic compounds are considered as a serious threat since they are not only toxic but also carcinogenic and harmful to all living organisms even at low concentrations. Therefore, the US environmental protection agency (EPA) calls for lowering of phenol content in wastewaters to less than 1 ppm [4].

The conventional removal methods for phenolic compounds were utilized such as adsorption, oxidation, solvent extraction, precipitation, and ion-exchange. Adsorption of phenol by activated carbon has proven to be effective, environmentally friendly, cost-effective, and sustainable. Adsorption using activate carbon remains the most widely used method for phenol removal due to the porous nature of interconnected pores, high adsorption capacity, favorable surface chemistry, and ionic nature of the carbon [1,5]. However, the application of activated carbon for phenols removal in aqueous media is hindered by the high cost of the commercial activated carbon which necessitates the development of a low-cost activated carbon for their removal. The use of agricultural waste materials such as oil palm shell seems to be promising because they are readily available, inexpensive, and can be regenerated. The use of such material as adsorbent help in solving their disposal challenge and at the same time producing a value added product [6,7]. However, a survey of the literature showed dearth of information concerning the use of ammonia for modification of oil palm shell-based activated carbon for the removal of phenol in an aqueous medium.

This study was carried out to prepare activated carbon from oil palm shell and also to modify it with aqueous ammonia so as to enhance its adsorption capacity. The characteristics of the activated carbon were explained by Scanning electron microscope (SEM), Fourier Transform Infrared spectroscopy (FTIR), BET surface area, and thermogravimetric analysis (TGA). A fixed-bed adsorption column was used for the study and column adsorption models such as Adams–Bohart, Thomas and Yoon–Nelson models were employed to provide insight into the adsorption characteristics, model fitting and adsorption capacity of the modified carbon.

2. Experimental

2.1. Reagents and instruments used

Merck chemicals Malaysia supplied potassium carbonate, aqueous ammonia (25%), and phenol. Nitrogen and carbon dioxide gas were purchased from Mega Mount Industrial Gases Sdn. Bhd, Johor Bahru, Malaysia. Oil palm shells were collected from Kian Hoe Plantations Sdn. Bhd., Kluang, Johor Bahru, Malaysia. The shells were washed with distilled water, then dried at 105˚C for 48 h, and was kept as the starting material for activated carbon production. The Stock solution of phenol was prepared by weighing and dissolving appropriate amount of phenol in 1,000 mL of deionized water. The solution pH of different initial phenol concentrations was adjusted using 0.1 M NaOH or HCl solutions to obtain desired pH values. The pH meter (UTECH instruments pH 700) was used to measure the solution pH. Also, UV–visible spectrometer (Perkin Elmer Spectrum-100) was used to determine the absorbance of the effluent phenol after passing through the fixed-bed column.

2.2. Procedures

2.2.1. Preparation of modified activated carbon

Two-step activation procedure was utilized for the activated carbon preparation from our previous study [6]. The precursor is first heated in an inert atmosphere resulting in the production of char that is then activated which helps to produce activated carbon with specific surface area. The raw material (oil palm shell) was first carbonized by heating in a furnace from ambient temperature to about 800˚C under an inert atmosphere of nitrogen flow of 150 cm^3/min for 2 h at 10˚C/min heating rate. The carbonized sample was impregnated with K_2CO_3 at a ratio of 2:1 g/g of chemical activant to char. The mixture was dried for 24 h at 105˚C in a hot air oven before being loaded into the reactor. The mixture was then activated by further heat treatment at 700˚C for 1 h under CO_2 flow

of 150 cm^3/min [5]. The AC produced was cooled down to about 50˚C under nitrogen flow before removing it from the furnace. The resultant AC was then washed with 0.1 M HCl and with distilled water until the washing's pH is close to 7. The sample was designated as potassium carbonate-treated activated carbon (PCAC) and was stored in a desiccator until use.

2.2.2. Ammonia treatment

To improve the hydrophobic properties and subsequently increase the adsorption of the activated carbon produced, the potassium carbonate synthesized carbon (PCAC) was modified by treatment with ammonia which was labeled as PCAC-AM. The ammonia solution for the production of PCAC-AM was made using 6.6 M $NH_3{\cdot}H_2O$ as reported by Li et al. The carbon was soaked in ammonia solution at 70˚C for 2 h and was then placed on a rotation vibrator at 35˚C for 24 h. The PCAC-AM produced was separated from the solution and was washed with distilled water repeatedly to remove excess ammonia. The ammonia treatment caused the introduction of a significant amount of nitrogen groups onto the carbon surface by the elimination of surface oxygen functional groups [8].

2.2.3. Characterization of the adsorbent

The ultimate analysis was carried out using Perkin Elmer elemental analyzer to determine carbon (C), hydrogen (H), nitrogen (N), and oxygen (O). The proximate analysis was carried out with the aid of TGA to determine moisture, volatile matter, fixed carbon and ash content as the residue. The TGA was carried out by heating the carbon from ambient temperature to 900˚C at a heating rate of 10˚C under nitrogen gas flow of 10 mL/min. The parameters were obtained as the carbon decreases in weight with time until the temperature reaches 900˚C. The residue was considered as the ash content. The surface functionalities were determined using FTIR using Perkin Elmer Spectra-Two recorded from 4,000–400 cm^{-1}. Zeta potential analysis of the sample was carried out using Anton Paar Electrokinetic Analyzer (surPASS 3) measured at a pH range between 2 and 11.

The pore structure of the carbon was determined by adsorption of liquefied nitrogen at −196˚C to obtain isotherms that were used to get the surface area which was obtained using volumetric techniques (Micromeritics ASAP 2020). The surface area was calculated by the BET [9] method and the pore volume from the amount of nitrogen gas adsorbed at (P/P_0) = 0.99 [10]. SEM was applied to study the surface morphology of the carbon using JEOL JSM-7600F.

2.2.4. Column adsorption studies for phenol

The column adsorption studies were conducted at room temperature, atmospheric pressure, and constant pH of 6.5. The fixed-bed column was carried out in a glass column of 1.2 cm internal diameter and 19.5 cm length. Three bed-depths of 1, 2, and 3 cm were selected. Three parameters including initial phenol concentration, flow rate, and bed depths of the adsorbent were studied. Glass wool was used at the bottom as support for the activated carbon to avoid it from being washed away. The influent phenol solution with given flow rate of 3, 6, and 9 mL/min was pumped by the peristaltic pump to the top of the column. The effluent phenol solution was withdrawn after every 10 min and was examine by UV–visible spectrophotometer (Perkin–Elmer Spectrum-100) at 270 nm. The absorbance from the withdrawn effluent phenol solution was recorded in triplicates. The average in each case of the phenol absorbance was used to calculate the quantity of phenol adsorbed.

2.2.5. Column data analysis

Adsorption capacities and quantities are vital indicators for adsorbent performance in column test. Usually, breakthrough curves were used to show the performance of adsorbent in a fixed-bed column [11]. The breakthrough curve is expressed as C_t/C_0 as a function of time for a given set of conditions, where C_t is the initial phenol concentration, C_0 is the concentration of phenol after a given time [5]. The breakthrough point is the point that initial phenol concentration (C_t) reaches about 0.1% of its concentration at a given time (C_0) and that corresponding time is the breakthrough time (t_b). The exhaustion time (t_e) is reached when the concentration of phenol at a given time reaches 95% of its initial concentration. The mass of phenol adsorbed on the activated carbon could be calculated by the following equations:

$$q_{\text{total}} = \frac{QA}{1000} = \frac{Q}{1000}\int_{t=0}^{t=t_{\text{total}}} C_{\text{ad}}\,dt \tag{1}$$

where t_{total} is the total flow time (min), Q is the flow rate (mL/min), A is the area above the breakthrough curve, and C_{ad} (mg/L) is the adsorbed concentration.

Eq. (2) was used to calculate the total amount of phenol that flows through the column:

$$m_{\text{total}} = \frac{C_0\, Q t_{\text{total}}}{1000} \tag{2}$$

The equilibrium uptake or maximum capacity of the column q_e (mg/g) is calculated by Eq. (3):

$$q_e = \frac{q_{\text{total}}}{m} \tag{3}$$

where m is the dry weight of activated carbon in the column (g)

2.2.6. Modeling of column adsorption data

For the appropriate design of column, a good prediction of the breakthrough curve is needed. In this study, three well-known models were applied to fit the adsorption of phenol by the modified activated carbon which includes Adams–Bohart, Thomas, and Yoon–Nelson models.

2.2.7. Error analysis

Error analysis is utilized to confirm the model that best fit the adsorption process. This was carried out using Eqs. (4) and (5) below in combination with the values from correlation coefficient (R^2):

$$\text{Sum of squares (SS)} = \sqrt{\sum \frac{(y_e - y_c)^2}{n}} \tag{4}$$

where y_e and y_c are the experimental and calculated (expected) values, while n is the number of experimental data points [12,13].

$$\text{Relative mean square error (RMSE)} = \sqrt{\frac{\sum_{i=1}^{n}(y_{\text{pred}} - y_{\text{exp}})^2}{n}} \tag{5}$$

where y_{pred} and y_{exp} were the predicted (expected) and experimental values, and n represent the number of experimental data points [14,15].

2.2.8. Thermodynamic analysis

The values for thermodynamic parameters such as Gibb's free energy change (ΔG), enthalpy change (ΔH), and entropy change (ΔS) of the adsorption process were investigated in a batch mode by agitation of 0.1 g the adsorbent in 50 mL solution of 50 mg/L and 250 phenol at different temperatures of 30, 40, and 50°C. Other parameters of the process were pH 6.5 can be deduced from the Eqs. (4)–(7):

$$K_c = \frac{(C_i - C_e)V}{(C_i \cdot m)} \tag{6}$$

$$\Delta G = -RT \ln K_c \tag{7}$$

$$\Delta G = \Delta H - T\Delta S \tag{8}$$

Then,

$$\ln K_c = -\frac{\Delta H}{RT} + \frac{\Delta S}{R} \tag{9}$$

This can also be rearranged as:

$$\ln K_c = -\frac{\Delta H}{R}\left(\frac{1}{T}\right) + \frac{\Delta S}{R} \tag{10}$$

where K is the amount of phenol adsorbed, R is the molar gas constant (8.314 J mol^{-1} K^{-1}), T is the absolute temperature (K). Whereas C_i, C_e, m, ΔG, ΔH, and ΔS are the initial phenol concentration, equilibrium phenol concentration, mass of adsorbent, changes in Gibb's free energy, enthalpy, and entropy, respectively [16–18]. The linear plot of $\ln K_c$ against $1/T$ gives the enthalpy change as the slope and change in entropy as the intercept as presented in Fig. 1.

3. Results and discussion

3.1. Characterization of adsorbent

3.1.1. Ultimate and proximate analysis

The ultimate analysis (as presented in Table 1) sheds light on the elemental composition of the

Table 1
Ultimate and proximate analysis

Ultimate analysis (%)		Proximate analysis (%)	
Carbon	52.11	Moisture	5.60
Hydrogen	5.73	Volatile	68.75
Nitrogen	1.82	Ash	2.38
Sulfur	0.00	Fixed carbon	23.27
Oxygen	40.34		

precursor material so as to ascertain its suitability for carbon synthesis (high carbon content of 52.11%), while proximate analysis in collaboration with TGA gives an insight into the volatile and fixed carbon contents of the precursor which help in selection of good starting material that will give better carbon yield [19].

3.1.2. Fourier transform infrared spectroscopy

The spectra of the raw precursor (RPS) as in Fig. 2, indicate bands at 621, 875, 1,033, 1,594, and 3,330 cm^{-1} that corresponds to bending in benzene derivatives, C–O–C stretching vibration, C–O stretching in ethers, C=C stretching in aromatic rings and OH stretching vibration in OH functional groups, respectively. However, the spectra also shows elimination of some peaks at 875, 1,594, and 3,330 cm^{-1} as a result of decomposition of functional groups and release of volatile matter during carbonization process. Also, peaks depicted at 620 and 3,882 cm^{-1} were introduced, which corresponds to OH stretching vibration (alcohols and phenols) and bending vibration from carbon-carbon triple bond or C–H bond from alkynes [20].

3.1.3. Brunauer–Emmett–Teller surface area and pore volume analysis

The most important property that determines its high adsorption is its adsorptive capacity which is directly proportional to the surface area [19]. The Brunauer–Emmett–Teller (BET) surface area and pore volume of PCAC is 707.8 m^2/g and 0.31 cm^3/g (as shown in Fig. 3). The results compare well with those obtained by Adinata et al [21] with surface area and pore volume of 1,170 m^2/g and 0.57 cm^3/g from palm

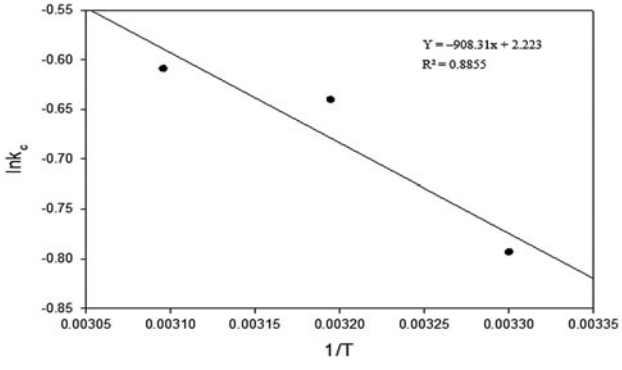

Fig. 1. Linear plot of ln K_c against $1/T$ at initial concentration of 50 mg/L, pH of 6.5, steering speed of 150 rpm, and adsorbent dose of 0.1 g.

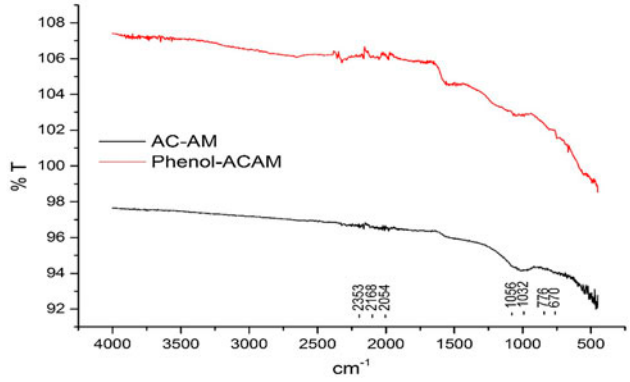

Fig. 2. FTIR spectra of modified (AC-AM) and phenol adsorbed (Phenol-ACAM) activated carbon.

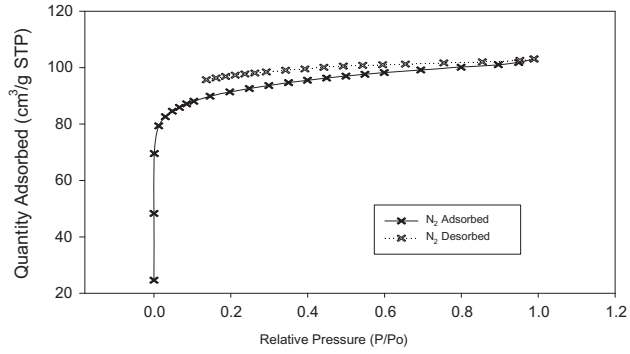

Fig. 3. Showing Type I isotherm plot from adsorption and desorption of nitrogen by PCAC.

oil shell precursor [21]. They showed that specific surface area increases from 600 to 800°C, decreases above 800°C, and the maximum surface area was obtained around 800°C. The PCAC composed of mainly pores in the region of micropores and is suitable for removal of organic contaminants in aqueous media [22].

3.1.4. Scanning electron microscopy

The SEM images show a significant difference between surface mophology of the materials [23] as shown in Fig. 4. It indicates that RPS is having no pores due to the presence of volatiles and other contaminants, but in (B) the pores start to form after carbonization. In (C) the pores were formed due to volatilization of contaminants and volatile matter, but in (D) some of the pores start to fold due to treatment with ammonia [8].

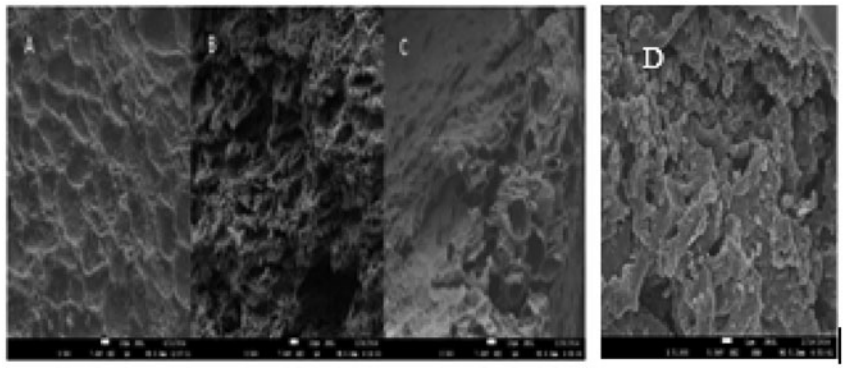

Fig. 4. Showing SEM images of (A) RPS, (B) CAC, (c) PCAC, and (PCAC-AM).

3.1.5. Zeta potential

The plot of zeta potential against the equilibrium solution pH was presented in Fig. 5. The isoelectric point value for the adsorbent was found to be 3.20 which indicated that the surface of the carbon is positive under pH 3.20 but negative above the value. The negative value increases up to pH 5 which indicated the region for lowest phenol adsorption due to repulsion. As the pH increases, the negative isoelectric point value decreases and the phenol adsorption increases as a result of less electrostatic repulsion between the adsorbent–adsorbate interaction [24].

3.2. Effects of column parameters

3.2.1. Effect of flow rate

The effect of solution flow rate for phenol adsorption was determined at different flow rates of (3, 6, and 9 mg/L), a constant bed depth of 3 cm, and initial phenol concentration of 50 mg/L (as presented in Fig. 6). The breakthrough curves for the fixed bed column were obtained by plotting C_t/C_0 (C_t and C_0 are effluent and influent BPA concentrations) against time (t). As can be seen from Fig. 2, the shorter breakthrough time was obtained at high flow rates. These is because a larger volume of water passed through the bed at higher flow rate. As a result, more phenol contacted with the accessible pores of the AC, making the pores get saturated rapidly. Conversely, higher adsorption capacity was observed at lower flow rate because lower flow rate enabled phenol to have more residence time in the column. Since phenol had longer contact time with the AC, equilibrium can be reached before it moved out of the column [25]. These results agree with the previous findings conducted by Wang et al. [26].

3.2.2. Effect of initial phenol concentration

The effect of initial phenol concentrations of 50 and 250 mg/L was studied at constant flow rate of 6 ml/L and a bed height of 3 cm (as presented in

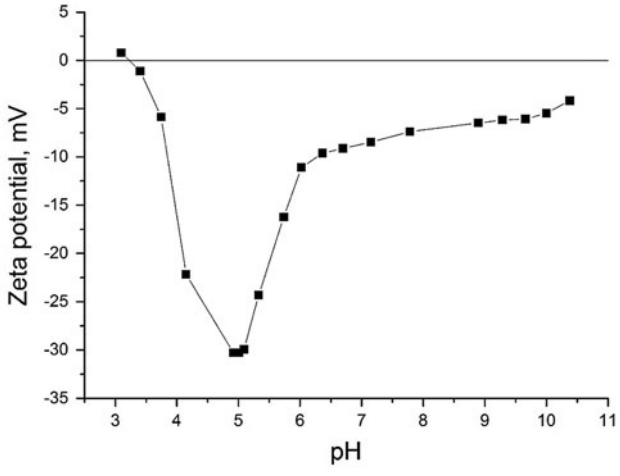

Fig. 5. Zeta potential for the modified activated carbon.

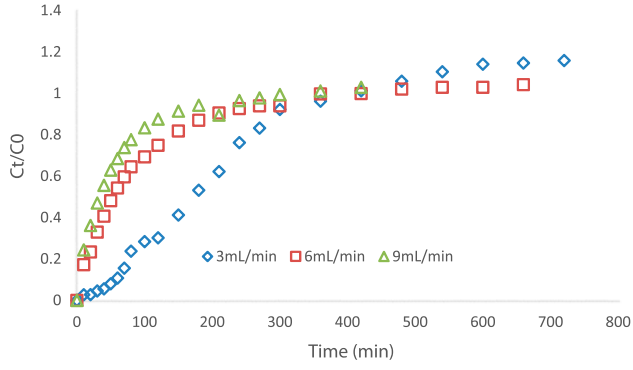

Fig. 6. Effect of flow rate at bed depth of 3 cm and 50 mg/L concentration.

Fig. 7). The extended breakthrough curve was observed at 50 mg/L with exhaustion time of 660 min. While at 250 mg/L concentration, the breakthrough curve declined with consequent fall of the exhaustion time of 360 min. The differences were due to lower concentration gradient leading to lower transport in the mass transfer coefficient of phenol in 50 mg/L, while 250 mg/L having larger phenol concentration became more quickly saturated in the column. A similar result was reported as the exhaustion point for o-xylene after ammonia treatment was observed at 200 min [8].

3.2.3. Effect of bed depth

Fig. 8 described the effect of bed height on the breakthrough curve of BPA adsorption onto AC. As can be seen, the figure has a steep breakthrough curve or shorter breakthrough time occurred at low bed height. At 3, 2, and 1 cm bed heights, the breakthrough curve becomes shorter and the breakthrough time (540, 300, and 120 mins, respectively) becomes smaller. These were due to the presence of fewer adsorption sites for the phenol to be adsorbed. As bed height increases, more sites are available for adsorption and the breakthrough curve becomes inclined while the breakthrough time becomes larger. However, Paudyal et al. suggested that the effect of shorter breakthrough curve could be minimized by increasing the column diameter [27].

3.3. Breakthrough curves modeling

The prediction of the breakthrough curves is vital for designing column studies because it provides a good understanding of the adsorbent surface properties, affinity, and adsorption pathways [25]. For this reason, various models were utilized to explain the dynamic adsorption behavior of the modified

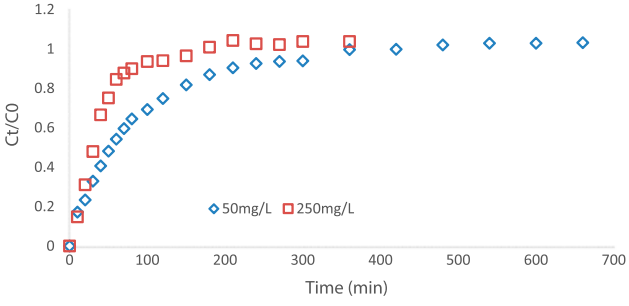

Fig. 7. Effect of initial phenol concentration at constant bed height of 3 cm and flow rate of 6 ml/L.

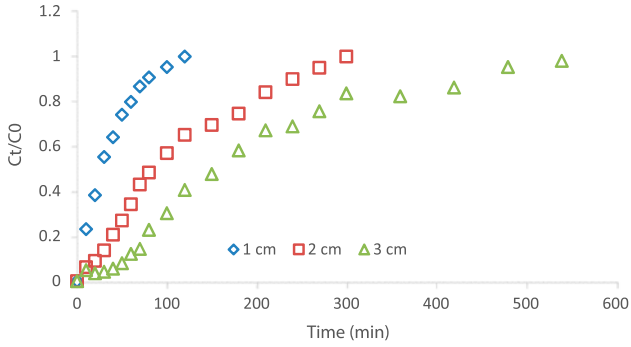

Fig. 8. Effect of bed depth at constant concentration of 50 mg/L and flow rate of 6 mL/min.

activated carbon. The models include Adams–Bohart, Thomas, and Yoon–Nelson.

3.3.1. Adams–Bohart model

This model assumes an instantaneous equilibrium and the adsorption rate is controlled by external mass transfer. The model is useful for analyzing initial part of breakthrough curves when $C_t/C_0 = 0$–0.5 [29]. The equation of the model is expressed as:

$$\ln\frac{C_t}{C_0} = K_{AB}C_0t - K_{AB}N_0\frac{Z}{Y} \tag{11}$$

where C_0 and C_t (mg/L) are the concentration of the influent and effluent phenol, K_{AB} (L/mg min) is the kinetic constant, N_0 (mg/L) is the column saturation constant, Z [28] is the bed height, and F (cm/min) is the linear velocity obtained from division of flow rate by the column section area (cm^2).

From the model equation, K_{AB} and N_0 can be estimated by plotting $\ln(C_0/C_t)$ against t. As presented in Table 1 above, the adsorption capacity of the column (N_0) decreased from −62.2 to −605.11 with increasing flow rate from 3 to 9 mL/min. On the other hand, N_0 values increased from −605.11 to −2.6 when the bed depth was increased from 1 to 3 cm. The increase in initial phenol concentration from 50 to 250 mg/L led to increase in N_0 from −2.46 to −1.51 mg/L. The model rate constant declined from 55,555.56 to 14,705.88 L/(mg min) with increasing bed depth. The results showed that better adsorption of the column can be achieved with higher initial phenol concentration, higher bed depth, and lower feed flow rate [30]. The number of correlation coefficients for a serial set of experiments greater than 0.9 obtained from this model was very low in proportion (1/9) of the adsorption test. Also, the correlation coefficient, RMSD, and

SS of the model are 0.9991, 14.18, and 1.98, respectively. Therefore, it shows that Adams–Bohart model cannot provide a good fit to the adsorption of phenol on the modified carbon.

3.3.2. Thomas model

Thomas model was developed based on two assumptions, that adsorption is not limited to only chemical interactions but also by mass transfer at the interface and the adsorption experimental data follows Langmuir adsorption isotherms and as well second-order kinetics. Contrary to Adams–Bohart model, Thomas model is suitable for characterizing the whole breakthrough curve [31]. The model in linear form can be represented by the equation below:

$$\ln\left(\frac{C_0}{C_t}-1\right)=K_{\mathrm{Th}}q_0\frac{m}{Q}-K_{\mathrm{Th}}C_0t \tag{12}$$

where K_{Th} is for Thomas rate constant (mL/min mg), q_0 is the adsorption capacity (mg/g), C_0 is the influent phenol concentration (mg/L), C_t is the effluent phenol concentration (mg/L), m is the mass of adsorbent (g), Q is the feed flow rate (mL/min), and t is the filtration time (min). The values of K_{Th} and q_0 were estimated from the linear plot of $\ln(C_0/C_t-1)$ against t and were shown in Table 2.

As the feed flow rate increase from 6 to 9 mL/min, the rate constant increased from −22,666 to −116 mL/(min mg) and as a result of that, the adsorption capacity reduced from −267.46 to −808.39. An increase in initial phenol concentration from 50 to 250 mg/L leads to elevation of both Thomas model rate constant and (−2.50 to −1.50 mL/(min mg)) and adsorption capacity (−10,737.10 to 2,922.76 mg/g). Elevation of bed depth from 1 to 3 cm resulted in a decrease of the model constant from −808.39 to −10,737.10 mL/(min mg). Higher adsorption capacity at higher initial phenol concentration can be attributed to large concentration gradient and higher driving force [27].

The number of correlation coefficients greater than 0.9 from this model's adsorption test is (7/9). Also, the model has individual correlation coefficient, RMSD and SS of 0.9913, 47.57, and 40.51. Thomas model cannot provide a good fit for the adsorption studies even though it has a high number of tests with R^2 greater than 0.9, but is has lower R^2 for the individual model, high RMSD, and SS when compared with Yoon–Nelson model.

3.3.3. Yoon–Nelson model

The Yoon–Nelson model is similar to Thomas model. The model can moderate the limitations of Adams–Bohart model at the latter part of the breakthrough curve. The linear form of the model is given by:

Table 2
Adams–Bohart, Thomas, and Yoon–Nelson model constants for the phenol adsorption by modified activated carbon packed column

Conditions				Adams–Bohart			Thomas			Yoon–Nelson		
pH	Q	Z	C_i	K_{AB}	N_0 (10^{-5})	R^2	K_{Th} (10^{-5})	q_o	R^2	K_{YN}	τ	R^2
6.5	3	1	50	4,385.9	−62.2	0.743	−116	−4,819.17	0.9227	0.057	32.12	0.9227
6.5	6	1	50	3,571.42	−93.66	0.9188	−22,666	−267.46	0.9636	10.104	1.12	0.9636
6.5	9	1	50	4,464.28	−605.11	0.8103	−370	−808.39	0.9768	0.185	−1.79	0.9768
6.5	3	2	50	6,410.25	−3.65	0.721	−4.50	−8,150.88	0.8893	0.0227	−106.90	0.8893
6.5	3	3	50	8,196.72	−2.46	0.6941	−2.50	−10,737.10	0.9106	0.0124	−214.74	0.9106
6.5	3	1	250	55,555.56	−1.51	0.4148	−1.50	2,922.76	0.439	0.0391	−142.35	0.8207
6.5	3	2	250	14,705.88	−18.95	0.6164	−17	−24,197.50	0.9355	0.0433	−64.52	0.9355
6.5	6	2	250	83,333.33	−0.92	0.7964	−9.70	54,956.79	0.9713	0.0243	73.27	0.7964
6.5	9	2	250	39,062.50	−3.005	0.8423	−0.50	−3,609.82	0.9901	0.126	−3.20	0.9901
RMSD				14.18			47.57			1.62		
SS (%)				1.95			40.51			40.51		
R^2				0.9991			0.9913			0.9993		

Notes: Q is the feed flow rate (mL/min); Z bed depth [28]; C_i initial phenol concentration (mg/L); K_{AB} Adams–Bohart rate constant (L/mg min); N_0 saturation concentration (mg/L); K_{Th} Thomas model rate constant (mL/mg min); q_o equilibrium phenol sorption capacity constant (mg/g); K_{YN} Yoon–Nelson model rate constant (1/min); τ time required for 50% breakthrough (min).

$$\ln\left(\frac{C_t}{C_0 - C_t}\right) = K_{YN}t - \tau K_{YN} \quad (13)$$

where K_{YN} is the Yoon–Nelson rate constant (min^{-1}) and τ is the required time for 50% phenol breakthrough (min). This parameters can estimated by plotting $\ln(C_t/C_0 - C_t)$ against t (min).

From Table 1, it is found that K_{YN} increased from 0.057 to 10.104 (min^{-1}) while τ decreased from 32.12 to 1.12 with an increase in feed flow rate (3–6 mL/min). Similar pattern was observed with increase in phenol concentration which is due to faster saturation of the column at high floe rate and high initial phenol concentration [29]. However, the model resulted in high correlation coefficients above 0.9 (6/9) for the adsorption tests, high R^2 for the individual model, and have the least RMSD (1.62) which indicates it was more satisfactory than both Adams–Bohart and Thomas models to fit and describe the phenol-modified carbon adsorption system.

3.4. Adsorption thermodynamics

3.4.1. Effect of temperature

The solution temperature plays a major role in adsorption processes. First of all, as the adsorbate temperature rises, the viscosity of the solution decreases which results in an increase in the diffusion rate of the adsorbate molecules on the surface of the adsorbent and this translates to higher adsorption (as presented in Fig. 9). Secondly, change in temperature may affect the equilibrium adsorption capacity of the adsorbent. The adsorption capacity reduces when the temperature is raised for an exothermic reaction and the opposite reaction takes place for endothermic reactions.

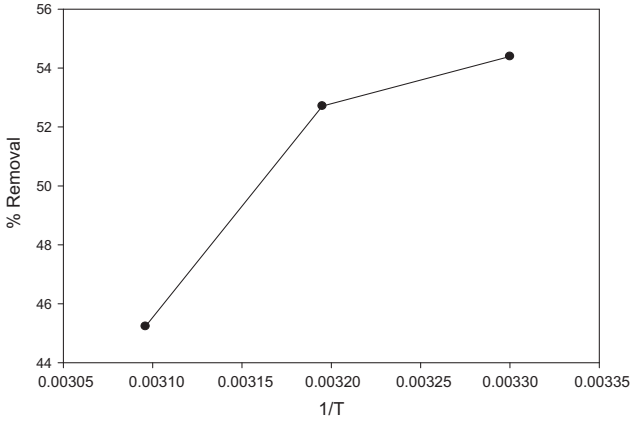

Fig. 9. The effect of temperature on the removal of phenol at initial concentration of 50 mg/L, pH of 6.5, steering speed of 150 rpm, and adsorbent dose of 0.1 g.

As can be seen from Fig. 9, the phenol adsorption onto the modified activated carbon increases with temperature. Therefore, this increase implied that the adsorption process is endothermic. This was due to the tendency of the phenolic molecules to be more adsorbed on the adsorbent surface from the aqueous solution through enhancement of the adsorptive forces between the phenol and the active sites as the temperature appreciates [32]. A similar finding was reported by Subash et al. in adsorption of phenol using garlic peel as the adsorbent [33].

3.4.2. Determination of free energy change (ΔG), enthalpy change (ΔH), and entropy change (ΔS)

An investigation of the effect of temperature on adsorption process gives a hint about ΔG, ΔH, and ΔS variations in relation with the adsorption [34]. In this study, experiments were carried out to find the optimum thermodynamic conditions on the adsorption of phenol onto ammonia-modified activated carbon at different temperatures of 303, 313, and 323 K. The results for the thermodynamic parameters of phenol adsorption are presented in Table 3.

From the results, it can be deduced that ΔG values are positive for all the temperatures which indicate the non-spontaneous nature of the adsorption process. The negative values of ΔG reduced with an increase in temperature, proving that the adsorption was better attained at higher temperatures. Also, the positive value of ΔH shows that the adsorption process is endothermic in nature. In addition, the ΔS negative value indicated less randomness of the adsorbent–adsorbate interface during the adsorption process. The negative value for ΔS (−18.5 kJ mol^{-1} K) can be linked to the movement of water molecules adsorbed by the adsorbate and which indicates that the surface of the adsorbent does not prefer phenol molecules over the adsorbed water molecules [33,35–37].

Table 3
Thermodynamic parameters of phenol adsorption onto modified activated carbon

T (K)	ΔG (kJ mol^{-1})	ΔH (kJ mol^{-1})	ΔS (kJ mol K)
303	1,998.5	7,551.7	−18.5
313	1,666.4		
323	1,635.3		

3.4.3. Estimation of activation energy

Knowledge about the magnitude of activation energy could give the type of adsorption that can be obtained. There are two kinds of adsorption, which are physical and chemical adsorption. Physisorption is characterized by mainly low activation energy (5–40 kJ mol^{-1}), while chemisorption requires higher activation energies (40–800 kJ mol^{-1}). However, activation energy is considered as non-activated chemical adsorption when its value is close to zero [34].

The activation energy for the phenol adsorption was deduced from Arrhenius equation given by:

$$K_2 = Ae^{\frac{-E_a}{RT}} \tag{14}$$

This linear form of the above equation can presented as:

$$\ln K_2 = -\frac{E_a}{RT} + \ln A \tag{15}$$

where K_2, R, A, T, and E_a stands for second-order rate constant, gas constant (8.314 kJ mol^{-1}), Arrhenius factor (g mg^{-1} min^{-1}), absolute temperature (K), and apparent activation energy (kJ mol^{-1}), respectively [16,18,38–40].

A plot of $\ln K_2$ against $1/T$ gives a straight line and the value of the activation energy is estimated from the slope ($-E_a/R$) as presented in Fig. 10. The activation energy was found to be 28 kJ mol^{-1} for the phenol adsorption. As mentioned above, in physisorption equilibrium is rapidly achieved and the process is reversible as the amount of energy required is small.

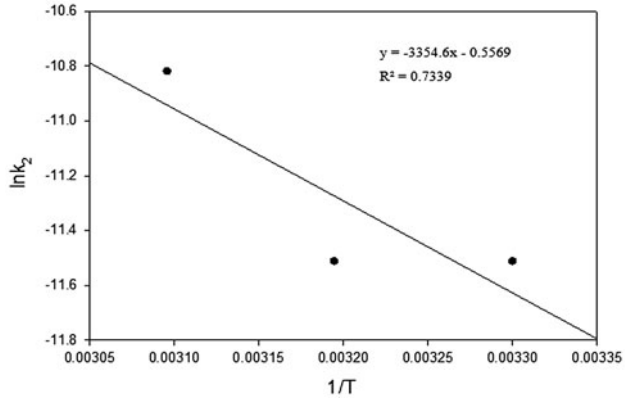

Fig. 10. Linear plot of $\ln K_2$ against $1/T$ at initial concentration of 50 mg/L, pH of 6.5, steering speed of 150 rpm, and adsorbent dose of 0.1 g.

3.5. Adsorption mechanism

Understanding the basic mechanism of phenol adsorption on the modified activated carbon is essential in evaluation of its behavior in the environment. It is known that the oxidation of activated carbon surfaces has a high impact on the removal of phenol, but is even more pronounced in the activated carbons with hydrophobic surfaces [41].

Fig. 2 shows the FTIR spectra of the modified activated carbon before and after adsorption of phenol. The C–O, C–N, and H streching vibrations peaks at 1,056, 1,032, and 670 cm^{-1} which disappear after phenol adsorption [42]. The peak at 776 cm^{-1} indicates the presence of aromatic –CH group and this confirm the adsorption of phenol by the AC [43]. This shows that the surface of the modified carbon played a role in phenol adsorption.

The dynamics of a biosorption process could also be described by either of the following:

(1) The removal of solutes from the bulk solution onto the adsorbent surface through the liquid film (film diffusion).
(2) The diffusion of the solute into the adsorbent's internal pores with a minute quantity of adsorption on the external surface (pore diffusion).
(3) The adsorption of the solute onto the internal surfaces and capillary spaces of the adsorbent [44–46]. Of the three steps, the third is assumed to be fast and negligible.

One of the commonly used ways to determine the mechanism involved in the biosorption is by determination of the activation energy of the process. Adsorption process is classified as film diffusion controlled when the E_a is below 16 kJ mol^{-1}, particle diffusion controlled when the E_a is between the range of 16–40 kJ mol^{-1}, and chemical reaction controlled when the E_a is above 40 kJ mol^{-1} [32]. The E_a of 28 kJ mol^{-1} value obtained in this study further validated the sorption of phenol on the modified activated carbon was pore diffusion controlled process.

4. Conclusions

This study explores the ability of modified palm shell-based carbon to remove phenol and its derivatives from water using fixed-bed adsorption mode.

The column adsorption performance was affected by adsorbent dosage, initial phenol concentration, and feed flow. The thermodynamic parameters revealed that the adsorption was non-spontaneous, endothermic, and pore diffusion controlled process. The maximum adsorption capacity of the carbon was 238.12 at 250 mg/L initial phenol concentration, 1 cm bed depth, and 9 mL/min flow rate. Adams–Bohart, Thomas and Yoon–Nelson models were used to fit experimental data, but only Yoon–Nelson model fitted well.

Acknowledgments

The authors would like to express appreciation to the office for research, innovation, commercialization, and consultancy management (ORICC) of University Tun Hussein Onn Malaysia for the financial support given to Abdurrahman Garba through postgraduate incentive scheme (VOT 1253). Also, the authors acknowledged Universiti Teknologi Malaysia (UTM) for providing financial assistance through the International Doctoral Fund (IDF) with VOT number 69878.J090703.5661.07326.

References

[1] U. Beker, B. Ganbold, H. Dertli, D.D. Gülbayir, Adsorption of phenol by activated carbon: Influence of activation methods and solution pH, Energy Convers. Manage. 51 (2010) 235–240.
[2] Y. Liu, M. Gao, Z. Gu, Z. Luo, Y. Ye, L. Lu, Comparison between the removal of phenol and catechol by modified montmorillonite with two novel hydroxyl-containing Gemini surfactants, J. Hazard. Mater. 267 (2014) 71–80.
[3] W. Wang, S. Pan, R. Xu, J. Zhang, S. Wang, J. Shen, Competitive adsorption behaviors, characteristics, and dynamics of phenol, cresols, and dihydric phenols onto granular activated carbon, Desalin. Water Treat. 56 (2014) 770–778.
[4] Y. Park, G.A. Ayoko, R. Kurdi, E. Horváth, J. Kristóf, R.L. Frost, Adsorption of phenolic compounds by organoclays: Implications for the removal of organic pollutants from aqueous media, J. Colloid Interface Sci. 406 (2013) 196–208.
[5] J. Mohammed, N.S. Nasri, M.A.A. Zaini, U.D. Hamza, H.M. Zain, F.N. Ani, Optimization of microwave irradiated-coconut shell activated carbon using response surface methodology for adsorption of benzene and toluene, Desalin. Water Treat. 57 (2016) 7881–7897.
[6] A. Garba, H. Basri, N.S. Nasri, Preparation and characterization of green porous palm shell based activated carbon by two step chemical activation using KOH, Appl. Mech. Mater. 773–774 (2015) 1127–1132.
[7] J. Dasgupta, A. Kumar, D.D. Mandal, T. Mandal, S. Datta, Removal of phenol from aqueous solutions using adsorbents derived from low-cost agro-residues, Desalin. Water Treat. 57 (2015) 1–25.
[8] L. Li, S. Liu, J. Liu, Surface modification of coconut shell based activated carbon for the improvement of hydrophobic VOC removal, J. Hazard. Mater. 192 (2011) 683–690.
[9] D. Kalderis, S. Bethanis, P. Paraskeva, E. Diamadopoulos, Production of activated carbon from bagasse and rice husk by a single-stage chemical activation method at low retention times, Bioresour. Technol. 99 (2008) 6809–6816.
[10] N.S. Nasri, U.D. Hamza, S.N. Ismail, M.M. Ahmed, R. Mohsin, Assessment of porous carbons derived from sustainable palm solid waste for carbon dioxide capture, J. Cleaner Prod. 71 (2014) 148–157.
[11] J.-L. Gong, Y.-L. Zhang, Y. Jiang, G.-M. Zeng, Z.-H. Cui, K. Liu, Continuous adsorption of Pb(II) and methylene blue by engineered graphite oxide coated sand in fixed-bed column, Appl. Surf. Sci. 330 (2015) 148–157.
[12] A.F. Elsheikh, U.K. Ahmad, Z. Ramli, Removal of humic acid from water by adsorption onto dodecyltrimethylammonium bromide-modified zeolite in a fixed bed reactor, Desalin. Water Treat. 57 (2016) 8302–8318.
[13] R. Han, L. Zou, X. Zhao, Y. Xu, F. Xu, Y. Li, Y. Wang, Characterization and properties of iron oxide-coated zeolite as adsorbent for removal of copper(II) from solution in fixed bed column, Chem. Eng. J. 149 (2009) 123–131.
[14] M.S. Podder, C.B. Majumder, Studies on the removal of As(III) and As(V) through their adsorption onto granular activated carbon/$MnFe_2O_4$ composite: Isotherm studies and error analysis, Compos. Interfaces 23 (2016) 327–372.
[15] F.N. Azad, M. Ghaedi, A. Asfaram, A. Jamshidi, G. Hassani, A. Goudarzi, Optimization of the process parameters for the adsorption of ternary dyes by Ni doped FeO(OH)-NWs–AC using response surface methodology and an artificial neural network, RSC Adv. 6 (2016) 19768–19779.
[16] S. Yao, J. Zhang, D. Shen, R. Xiao, S. Gu, M. Zhao, Removal of Pb(II) from water by the activated carbon modified by nitric acid under microwave heating, J. Colloid Interface Sci. 463 (2016) 118–127.
[17] G. Zhang, T. Yan, D. Wei, L. Yan, X. Wang, Q. Wei, Anaerobic granular sludge-derived activated carbon: Preparation, characterization and superior dye adsorption capacity, Desalin. Water Treat. (2016) 1–12.
[18] G. Zhou, J. Luo, C. Liu, L. Chu, J. Ma, Y. Tang, A highly efficient polyampholyte hydrogel sorbent based fixed-bed process for heavy metal removal in actual industrial effluent, Water Res. 89 (2016) 151–160.
[19] N.S. Nasri, M. Jibril, M.A.A. Zaini, R. Mohsin, H.U. Dadum, A.M. Musa, Synthesis and characterization of green porous carbons with large surface area by two step chemical activation with KOH, J. Teknologi (Sci. Eng.) 67(4) (2014) 25–28.
[20] S. Sumathi, S. Chai, A. Mohamed, Utilization of oil palm as a source of renewable energy in Malaysia, Renewable Sustainable Energy Rev. 12 (2008) 2404–2421.
[21] D. Adinata, W.M. Wandaud, M.K. Aroua, Preparation and characterization of activated carbon from palm shell by chemical activation with K_2CO_3, Bioresour. Technol. 98 (2007) 145–149.

[22] X. Lu, J. Jiang, K. Sun, X. Xie, Y. Hu, Surface modification, characterization and adsorptive properties of a coconut activated carbon, Appl. Surf. Sci. 258 (2012) 8247–8252.
[23] J. Cruz-Olivares, C. Pérez-Alonso, C. Barrera-Díaz, F. Ureña-Nuñez, M. Chaparro-Mercado, B. Bilyeu, Modeling of lead (II) biosorption by residue of allspice in a fixed-bed column, Chem. Eng. J. 228 (2013) 21–27.
[24] S. Hong, S. Deng, X. Yao, B. Wang, Y. Wang, J. Huang, Bromate removal from water by polypyrrole tailored activated carbon, J. Colloid Interface Sci. 467 (2016) 10–16.
[25] T. Nguyen, H. Ngo, W. Guo, T. Pham, F. Li, T. Nguyen, Adsorption of phosphate from aqueous solutions and sewage using zirconium loaded okara (ZLO): Fixed-bed column study, Sci. Total Environ. 523 (2015) 40–49.
[26] W. Wang, M. Li, Q. Zeng, Adsorption of chromium (VI) by strong alkaline anion exchange fiber in a fixed-bed column: Experiments and models fitting and evaluating, Sep. Sci. Technol. 149 (2015) 16–23.
[27] H. Paudyal, B. Pangeni, K. Inoue, H. Kawakita, K. Ohto, S. Alam, Adsorptive removal of fluoride from aqueous medium using a fixed bed column packed with Zr(IV) loaded dried orange juice residue, Bioresour. Technol. 146 (2013) 713–720.
[28] K.Y. Nelson, D.W. McMartin, C.K. Yost, K.J. Runtz, T. Ono, Point-of-use water disinfection using UV light-emitting diodes to reduce bacterial contamination, Environ. Sci. Pollut. Res. 20 (2013) 5441–5448.
[29] R. Sharma, B. Singh, Removal of Ni (II) ions from aqueous solutions using modified rice straw in a fixed bed column, Bioresour. Technol. 146 (2013) 519–524.
[30] D. Bulgariu, L. Bulgariu, Sorption of Pb(II) onto a mixture of algae waste biomass and anion exchanger resin in a packed-bed column, Bioresour. Technol. 129 (2013) 374–380.
[31] A. Katsigiannis, C. Noutsopoulos, J. Mantziaras, M. Gioldasi, Removal of emerging pollutants through granular activated carbon, Chem. Eng. J. 280 (2015) 49–57.
[32] R.-L. Liu, Y. Liu, X.-Y. Zhou, Z.-Q. Zhang, J. Zhang, F.-Q. Dang, Biomass-derived highly porous functional carbon fabricated by using a free-standing template for efficient removal of methylene blue, Bioresour. Technol. 154 (2014) 138–147.
[33] N. Subash, R. Krishna Prasad, Kinetics and mass transfer models for sorption of titanium industry effluent in activated carbon, Desalin. Water Treat. 57 (2016) 7254–7261.
[34] E. Cheraghi, E. Ameri, A. Moheb, Continuous biosorption of Cd(II) ions from aqueous solutions by sesame waste: Thermodynamics and fixed-bed column studies, Desalin. Water Treat. 57 (2016) 6936–6949.
[35] N.G. Rincón-Silva, J.C. Moreno-Piraján, L. G. Giraldo, Thermodynamic study of adsorption of phenol, 4-chlorophenol, and 4-nitrophenol on activated carbon obtained from eucalyptus seed, J. Chem. 2015 (2015) 1–12.
[36] N.G. Rincón-Silva, J.C. Moreno-Piraján, L. Giraldo, Equilibrium, kinetics and thermodynamics study of phenols adsorption onto activated carbon obtained from lignocellulosic material (Eucalyptus Globulus labill seed), Adsorption 22 (2016) 33–48.
[37] R.I. Yousef, B. El-Eswed, H. Ala'a, Adsorption characteristics of natural zeolites as solid adsorbents for phenol removal from aqueous solutions: Kinetics, mechanism, and thermodynamics studies, Chem. Eng. J. 171 (2011) 1143–1149.
[38] N. Douara, B. Bestani, N. Benderdouche, L. Duclaux, Sawdust-based activated carbon ability in the removal of phenol-based organics from aqueous media, Desalin. Water Treat. 57 (2016) 5529–5545.
[39] M. Khan, S. Akhtar, S. Zafar, A. Shaheen, M. Khan, R. Luque, Removal of congo red from aqueous solution by anion exchange membrane (EBTAC): Adsorption kinetics and themodynamics, Materials 8 (2015) 4147.
[40] E. Bilgin Simsek, B. Aytas, D. Duranoglu, U. Beker, A.W. Trochimczuk, A comparative study of 2-chlorophenol, 2,4-dichlorophenol, and 2,4,6-trichlorophenol adsorption onto polymeric, commercial, and carbonaceous adsorbents, Desalin. Water Treat. 57 (2016) 9940–9956.
[41] L.F. Velasco, C.O. Ania, Understanding phenol adsorption mechanisms on activated carbons, Adsorption 17 (2011) 247–254.
[42] N.T. Abdel-Ghani, G.A. El-Chaghaby, F. Helal, Preparation, characterization and phenol adsorption capacity of activated carbons from African beechwood sawdust, Global J. Environ. Sci. Manage. (in press).
[43] P. Muthamilselvi, R. Karthikeyan, B.S.M. Kumar, Adsorption of phenol onto garlic peel: Optimization, kinetics, isotherm, and thermodynamic studies, Desalin. Water Treat. 57 (2016) 2089–2103.
[44] R.K. Prasad, S. Srivastava, Sorption of distillery spent wash onto fly ash: Kinetics, mechanism, process design and factorial design, J. Hazard. Mater. 161 (2009) 1313–1322.
[45] A. Singhal, P.K. Jha, I.S. Thakur, Biosorption of pulp and paper mill effluent by *Emericella nidulans*: Isotherms, kinetics and mechanism, Desalin. Water Treat. (2016) 1–16.
[46] B.H. Hameed, I.A.W. Tan, A.L. Ahmad, Adsorption isotherm, kinetic modeling and mechanism of 2,4,6-trichlorophenol on coconut husk-based activated carbon, Chem. Eng. J. 144 (2008) 235–244.